Distribution of electrons in double photoionization of helium and heavier atoms in the asymptotic region

E. G. Drukarev
Petersburg Nuclear Physics Institute, Gatchina, St. Petersburg 188350, Russia
(Received 13 April 1994; revised manuscript received 13 April 1995)

This paper presents an analysis of the energy distribution of the outgoing electrons in the double ionization of helium by photons with energies much larger than the ionization potential. The analysis improves on the one carried out by Amusia *et al.* [J. Phys. B **8**, 1248 (1975)] in the framework of the special model for the wave function of helium. Now the energy distribution is expressed through certain expectation values averaged over the initial state described by the wave function of the general form $\Psi(r_1,r_2)$. A larger interval of values of photon energies is considered. The limit equations for the angular distribution are obtained. The general features of the process with heavier atoms are also analyzed.

PACS number(s): 32.80.Fb, 32.70.Cs, 32.30.Rj

I. INTRODUCTION

In recent years interest in the problem of double photoionization of helium has been renewed. The experimental facilities developed and the investigation of the processes caused by photons as energetic as 12 keV became possible [2]. Physicists are interested now by such problems as the relative roles of ground state and final state interactions (GSI and FSI) [3,4], the energy and the angular distribution of the outgoing electrons [5–9], the breakdown of asymptotics at large and small energies [7,10], the role of the Compton scattering in formation of doubly charged ions [11–13], the connection of the cross section to that of other processes [10], etc. The earlier papers are reviewed in [14].

In this paper we investigate the energy and angular distribution of outgoing electrons at large values of photon energies ω (corresponding, however, to nonrelativistic energies of outgoing electrons)

$$J \ll \omega \ll m \tag{1}$$

with J standing for the ionization potential and m the mass of the electron. We expect also that the results obtained will help us to solve the other problems in the field discussed nowadays.

It was shown in Ref. [1] that there are three possible mechanisms of double photoionization. Each of them dominates in a certain part of the spectrum. If one of the electron's energies is $\epsilon_1 \sim \omega$, while $\epsilon_2 \sim J$, the well-known shake-off mechanism is at work [15]. When both ϵ_1 and ϵ_2 become much larger than J, but the difference $|\epsilon_1 - \epsilon_2|$ is not too small, the final state interaction mechanism dominates. In these two regions large momentum is transferred to the nucleus. However, if the difference of the energies of the outgoing electrons is small enough, the quasifree process with small momentum transferred to the nucleus determines the energy distribution. The concrete calculations in [1] were carried out in a special model of the initial state wave function which included the interaction between electrons in the lowest order of perturbation theory. Photon energies ω in the interval 1.5 keV $\ll \omega \ll$ 0.5 MeV were considered. The spectrum was calculated for several values of photon energies.

In the present paper we improve the analysis carried out in [1] mainly at two points. We describe the initial state by the general function $\Psi(r_1,r_2)$. We show that for $\epsilon_{1,2} \gg J$ the energy distribution in both regions can be presented as the product of "electrodynamical" and "atomic physics" factors. The former describes the interaction of two free electrons at different kinematics. The latter is expressed through expectation values of certain operators averaged over the ground state, containing all atomic physics effects. Also a larger interval of energies ($\omega \gg 50$ eV instead of $\omega \gg 1.5$ keV) is considered now. These two improvements enable us to follow the change in the shape of the spectrum curves with photon energy ω, matching the three singled-out regions of the spectrum. One more point is the limit equations for the angular distribution. We also discuss the general features of the process for heavier atoms.

Following Ref. [1] we describe the outgoing electrons with energies $\epsilon_{1,2} \gg J$ as well as the intermediate electrons by plane waves. The interaction between the two fast electrons is included in the first order of perturbative theory. Both approximations are true with relative accuracy $(J/\epsilon) \sim (J/\omega) \ll 1$. The initial electrons are described by a function of the general form $\Psi(r_1,r_2)$.

In the calculations carried out in [1] the initial state of the atom was described by a product of single-particle hydrogenlike functions. In the momentum space they are

$$\psi_h(f) = N_0 \frac{4\eta}{(f^2+4\eta^2)^2}, \tag{2}$$

being the Fourier components of the well known functions

$$\psi_h(r) = N_0 \exp(-r\eta), \quad N_0 = \psi_h(r=0). \tag{3}$$

The function presented by Eq. (2) explicitly provides the scale for momentum f, i.e.,

$$\left| \frac{\psi(f \gg \eta)}{\psi(f \sim \eta)} \right| \ll 1. \tag{4}$$

We use the relativistic units $\hbar = c = 1$, $e^2 = \alpha = 1/137$ (see the Appendix). In these units

$$\eta = m\alpha Z \tag{5}$$

with Z the charge of the nucleus. The main point of the analysis of the energy distribution was that the process yields large momentum $q \gg \eta$ to be transferred to the nucleus unless special kinematics is chosen. Indeed,

$$q = p_1 + p_2 - k \tag{6}$$

with p_i and k standing for the momenta of the outgoing electrons and that of the photon $[|p_i| = (2m\epsilon_i)^{1/2}, |k| = \omega]$. Equation (5) leads to $J = \eta^2/2m$, thus $|p_i| \gg \eta$ if $\epsilon_i \gg J$. Since only the initial state electrons interacted with the nucleus they transferred momentum q. Hence the amplitude contained a small factor $\psi_h(q)$—see Eq. (4). However, if both $\epsilon_{1,2}$ were close to the center of the energy distribution one could make $|p_1 + p_2| \ll p_{1,2}$. Thus the momentum q becomes smaller leading to a strong enhancement of the amplitude.

Here we present the result of an investigation of the spectrum which does not clarify the form of the initial state wave function. The basic point is that the wave function of an atom of helium $\Psi(r_1, r_2)$ is a superposition of the terms containing exponential factors of the form presented by Eq. (3) with $r = r_{1,2}$ or $r = |r_1 - r_2|$. Thus the existence of a scale for momenta $f_{1,2}$ for which Eq. (4) is true is the general feature of any function $\Psi(f_1, f_2)$ which is the Fourier component of $\Psi(r_1, r_2)$. This enables us to present the energy distribution as the superposition of terms of two types. In the first ones all the dependence on the energies ω and ϵ is singled out while all the dependence on the structure of the initial state enters through certain expectation values. The terms of the second type are the integrals over q of the distribution $d\sigma^{2+}/d\epsilon dq$. The latter is expressed through certain integrals over $r_{1,2}$. The integrals contain $\Psi(r_1, r_2)$ and certain functions explicitly depending on q and r_i. Thus there are two scales for the values of r_i. The first one is $r_i \sim q^{-1}$. The second one is determined by exponential factors of the form of Eq. (3). We can write that the second scale is $r_i \sim \eta_{eff}^{-1}$ with η_{eff} being a certain "effective" value of η. At $q \gg \eta_e$ the leading contribution to the integrals over r_i is determined by $r_i \sim q^{-1}$ and these terms are quenched. However, if the values of the energies of the outgoing electrons are close enough, i.e., if the value of the parameter

$$\beta = \frac{|\epsilon_1 - \epsilon_2|}{\omega} \tag{7}$$

is small enough, the values of $q \lesssim \eta_{eff}$ become available. The integrals are determined now by $r_i \sim \eta_{eff}^{-1}$, i.e., the values are determined by the structure of the initial state. Thus the possibility of making $q \lesssim \eta_{eff}$ at small values of β leads to strong enhancement of the distribution $d\sigma^{2+}/d\epsilon dq$ at $q \sim \eta_{eff}$. If the value of ω is large enough, the region $q \sim \eta_{eff}$ gives the leading contribution to $d\sigma^{2+}/d\epsilon$ if the value of β is small enough.

The "effective value" η_{eff} can be calculated for each special choice of the function $\Psi(r_1, r_2)$. But we need not do this since we present the contribution to $d\sigma^{2+}/d\epsilon$ by the explicit functions of β expressed through certain integrals containing $\Psi(r_1, r_2)$. The integrals provide large contributions if the values of β are small enough and vanish smoothly at $\beta \sim 1$. Note, however, that the latter should be of the same order of magnitude as those calculated with the hydrogenlike functions with $Z = Z_V = 27/16$ coming from the variation principle [16], i.e., we expect $\eta_{eff}/\eta \sim 1$, while

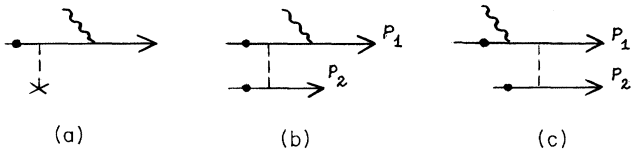

FIG. 1. Diagram describing single (a) and double (b) and (c) photoionization in the asymptotic region at $\epsilon_{1,2} \gg J$ for the double process. The wavy line shows the real photon. The dashed line presents the hard photon with $f \gg \eta$. The dark circles stand for photons with $f \sim \eta$ exchanged by bound electrons with the nucleus and with each other.

$$\eta = m\alpha Z_V = 6.3 \text{ keV}. \tag{8}$$

The reason is that the function $\Psi(r_1, r_2)$ at $r_{1,2} \sim \eta_{eff}^{-1}$ determines the value of the binding energy of the atom. The hydrogenlike model reproduces the latter value with the accuracy of about 2%. We shall present the values of several parameters in the framework of this model. In the general case we shall present the values also "in units" of η. Note also the value of the single-particle binding energy $J = \eta^2/2m$ and that of $N_0^2 = \eta^3/\pi$ in the hydrogenlike model.

The spectrum $d\sigma^{2+}/d\epsilon_2$ is shown to be dominated by a special part of the angular distribution of outgoing electrons. All the results can be generalized to the knockout of two electrons with the binding energy of the same order of magnitude from any multielectron system.

In Sec. II we shall recall the picture of the single photoeffect. In Sec. III we show qualitatively how the three parts of the spectrum emerge. In Secs. IV and V we present the energy distribution in the two parts of the spectrum of fast electrons. The general outlook of the energy distribution in helium is given in Sec. VI and for heavier atoms in Sec. VII. The angular distribution is discussed in Sec. VIII. Results are summarized in Sec. IX.

II. THE ASYMPTOTICS OF SINGLE-ELECTRON PHOTOIONIZATION

It is instructive to start with the asymptotics of this well known process. Since the energy of an outgoing electron $\epsilon_1 = p_1^2/2m = \omega - J \gg J$ the latter can be described by a plane wave and the amplitude of the single-electron photoionization is

$$F_\gamma = (4\pi\alpha)^{1/2} \frac{(ep_1)}{m} \psi(p_1 - k). \tag{9}$$

Here $k(e)$ stands for the momentum (vector of polarization) of the photon and ψ stands for the single-particle wave function in helium. Since $|p_1| \approx (2m\omega)^{1/2} \gg \eta$ the argument of the function ψ is much larger than η. The single photoionization thus yields large momentum $q = |p_1 - k| \gg \eta$ to be transferred to the recoil atom. This corresponds to the impossibility of the process with a free electron.

One can see from Fig. 1 that each interaction of the bound

electron with the recoil atom in which large momentum $q \gg \eta$ is transferred leads to a small factor q^{-4}. Thus the bound electron exchanges an infinite number of soft photons, carrying momenta $f \sim \eta$, with the recoil atom and one "hard" photon carrying momentum $q \approx p_1 \gg \eta$. The latter exchange takes place in the cell closest to the ionizing photon. Both electron and photon propagators give the factors $\sim q^{-2}$. The momentum q should be transferred directly to the nucleus, otherwise new small factors $\sim q^{-2}$ emerge. Thus we obtain for the amplitude of single photoionization at $\omega \gg J$

$$F_\gamma = \frac{(4\pi\alpha)^{1/2} 4\pi\alpha Z \times 2m}{p_1^4} \frac{(ep_1)}{m} N_0 \tag{10}$$

with $p_1 \approx (2m\omega)^{1/2}$, $N_0 = \Psi(r=0)$, and Z the charge of the nucleus.

Equation (10) can be obtained in a more formal way from the Lippman-Schwinger equation (see, e.g., [17])

$$\langle q|\psi\rangle = \int \frac{d^3q_1 d^3f}{(2\pi)^6} \langle q|G_0(J_1)|q_1\rangle\langle q_1|V|f\rangle\langle f|\psi\rangle \tag{11}$$

with G_0 the free electron propagator, V the self-consistent field in which the electron moves, and $J_1 = -J$. Since the large momentum $q_1 = q$ should be transferred to the nucleus directly, we immediately come to Eq. (10).

Substituting Eq. (10) into the expression for the cross section [18]

$$d\sigma^+(\omega) = \frac{\pi}{\omega}\delta(\epsilon_1 - \omega + J)|F_\gamma|^2 \frac{d^3p_1}{(2\pi)^3} \tag{12}$$

we present the well known asymptotics [16] in the form

$$\sigma^+(\omega) = \frac{2^9\pi^2}{3} Z^2 N_0^2 \left(\frac{m\alpha^2}{2\omega}\right)^{7/2} \frac{1}{\alpha^4 m^5} . \tag{13}$$

Here Z is the charge of the nucleus. Hence the asymptotics of the single photoeffect contains one model-dependent parameter—the value of N_0.

III. THE THREE REGIONS OF THE SPECTRUM

There are three regions in the spectrum with different mechanisms of the process [1]. We recall the analyses of [1], carried out in momentum space adding analyses in configuration space. Though the momentum space is more convenient for the analyses we show also how the results can be obtained from the general equation for the amplitude in configuration space.

$$F = \langle \Phi(r_1, r_2)|e^{i(kr_1)} i(\bar{e}\bar{\nabla}_1) + (1 \to 2)|\Psi(r_1, r_2)\rangle . \tag{14}$$

Here $\Psi(r_1, r_2)$ and

$$\Phi(r_1, r_2) = \frac{1}{\sqrt{2}}[\varphi_1(r_1)\varphi_2(r_2) + \varphi_2(r_1)\varphi_1(r_2)] \tag{15}$$

are the wave functions of initial and final states. The functions φ_i in Eq. (15) are the single-particle functions of continuum electrons with the energies ϵ_i. They are normalized as

$$\int d^3r \varphi_i(r)\varphi_j(r) = (2\pi)^3 \delta(\bar{p}_i - \bar{p}_j). \tag{16}$$

A. The edge region

One of the electrons is slow: $\epsilon_2 \sim J$. This region is well known to give the leading contribution to the cross section $\sigma^{2+}(\omega)$. Hence one of the electrons (say, the one with energy ϵ_1) can be described by a plane wave: $\varphi_1(r) = \exp(ipr)$. Thus the amplitude is

$$F = F_\gamma \langle \varphi_2(r)|\Psi(0,r)\rangle . \tag{17}$$

Here F_γ is the amplitude of the single photoeffect. The process yields large momentum $q \sim p_1 \gg \eta$ transferred to the nucleons. Thus the amplitude is quenched by a small factor η^4/q^4 contained in the amplitude F_γ. The overlap matrix element involved in Eq. (17) is the well known probe for the model of the ground state function Ψ [15].

Substitution of Eq. (17) into the expression for the cross section of the double photoionization

$$d\sigma^{2+}(\omega) = \frac{\pi}{\omega}\delta(\epsilon_1 + \epsilon_2 - \omega - J^{2+})|F|^2 \frac{d^3p_1}{(2\pi)^3} \frac{d^3p_2}{(2\pi)^3} \tag{18}$$

singles out the cross section of the single photoeffect $\sigma^+(\omega)$. The integral over ϵ_2 is saturated by $\epsilon_2 \sim J$ [the matrix element in Eq. (17) falls as ϵ_2^{-2} at $\epsilon_2 \gg J$]. It does not depend on ω and determines the coefficient of proportionality between $\sigma^{2+}(\omega)$ and $\sigma^+(\omega)$.

To estimate the role of the final state interactions it is sufficient to compare the diagrams describing the interaction of the electrons in the lowest order of perturbative theory [Figs. 1(b) and 1(c)]. Using the Coulomb gauge for the photon propagators one can see the ratio of the contributions to be determined by that of the electron propagators. Considering the problem in momentum space one immediately finds the FSI contribution [Fig. 1(c)] to be $\epsilon_2/\omega \sim J/\omega \ll 1$ times smaller than that of the GSI.

Note however that the division of the interaction into GSI and FSI is a conventional one since it depends on the gauge of the photon propagators describing the interaction (not to be confused with the term "gauge" used sometimes for the form of the dipole interaction between photon and electron). Really, adding the longitudinal terms to the photon propagator (see, e.g., [19]), one can replace part of the GSI into the FSI, and vice versa. We consider the problem in the Coulomb gauge, usual for atomic physics. Note that a similar picture emerges in the Feynman gauge.

B. The region of domination of the FSI

Here $\epsilon_{1,2} \gg J$ and $|\epsilon_1 - \epsilon_2|/\omega \sim 1$. The exchange of electrons by a hard photon, carrying momentum $p_2 \gg \eta$, can be taken into account in the lowest order of perturbative theory in both GSI and FSI graphs, Figs. 1(b) and 1(c).

Unless a special region of kinematical variables is chosen, the two graphs give a contribution of the same order. However, if the value of

$$P=|\bar{p}_1+\bar{p}_2| \tag{19}$$

is close to

$$p_0=(2m\omega)^{1/2}, \tag{20}$$

i.e.,

$$|P-p_0|\sim\eta\ll P,p_0, \tag{21}$$

the electron propagator in the graph of Fig. 1(c) is close to the mass shell and the contribution is increased by the factor $p_0^2/\eta^2\gg 1$ with respect of that of Fig. 1(b).

Now let us see how the picture emerges in configuration space analyses. Since $\epsilon_{1,2}\gg J$ the final state function can be built from the two plane waves interacting in lowest order of perturbative theory. Using Eq. (15) for the final state function we present the contribution as

$$F\sim\int d^3r_1d^3r_2d^3r_3[e^{-i(p_1r_3)-i(p_2r_2)}V(r_3-r_2)\times G_0(\omega;r_1-r_3)i(e\nabla_1)+(1\rightarrow 2)]\Psi(r_1,r_2). \tag{22}$$

The values of r_i which dominate in the integral (22) are determined by the power of the exponent. Since $G_0\sim e^{-ip_0|r_1-r_3|}$ we find all $r_i\sim p_0^{-1}$ for arbitrary values of $p_0,p_1,p_2\gg\eta$. Thus the integral is quenched by the small value of the three phase volumes.

However, if Eq. (21) is true and $r_2\approx r_3$ we find the exponents to contribute $\approx e^{-ip_0r_1}e^{i(p_0-P)r_2}$. Thus only the phase volumes d^3r_1 and $d^3(r_2-r_3)$ appear to be limited while $r_2\sim\eta^{-1}$. This increases the value of the integral.

The physical picture becomes quite clear [1]. The photon produces ionization at small distances $r_1\approx p_1^{-1}$ from the nucleus. Since $|r_3-r_1|\sim\eta^{-1}$ the electron passes through the atom, interacting with the second electron at the distances where most of the latter is concentrated.

Hence it is almost obvious that the energy distribution reproduces that of free electron-electron scattering and contains the cross section of the single photoeffect as a factor. In Sec. IV we prove the statements and determine the factor depending on the structure of the initial state which enters the energy distribution Eq. (37).

However, if the values of the energies become close, another mechanism of the process emerges.

C. The central region

Here $\epsilon_{1,2}\sim\omega$ and $|(\epsilon_1-\epsilon_2)/\omega|\ll 1$. In order to understand why this region is singled out we must recall that the Fourier component of the wave function of a bound electron $\Psi(f)$ is large if $f\sim\eta$ but obtains the small factor $(\eta/f)^2$ if $f\gg\eta$. Thus until the momentum transferred to the nucleus—see Eq. (6)—is large, one of the arguments of the wave function of helium in momentum space $\Psi(f_1,f_2)$ is large ($f\gg\eta$) and the amplitude is quenched.

However, in the vicinity of the center the value of momentum q can become of the order of η. Thus both electrons involved are at the distance of their largest concentration ($r_{1,2}\sim\eta$) and the amplitude increases. The distance between electrons is still $|r_1-r_2|\sim p_0^{-1}\ll\eta^{-1}$.

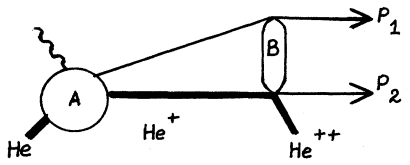

FIG. 2. The general form of the final state interaction. Block A stands for single photoionization; block B denotes ionization by electron impact.

Let us see how it looks in configuration space. Putting the plane waves as the functions φ_i in Eq. (15) and substituting into Eq. (14) we come to

$$F\sim\int d^3r_1d^3r_2[e^{i(kr_1)-i(p_1r_1)-i(p_2r_2)}i(e\nabla_1)+(1\rightarrow 2)]\Psi(r_1,r_2). \tag{23}$$

The exponential factor can be presented as $\exp[-i(qr_1)-i(p_2,r_1-r_2)]$. Thus at $q\sim\eta$ both r_1 and r_2 become of the order η^{-1} while $|r_1-r_2|$ is of the order $p_2^{-1}\ll\eta^{-1}$.

The condition $|q|\lesssim\eta$ becomes true if

$$\beta\equiv\begin{cases}\dfrac{|\epsilon_1-\epsilon_2|}{\omega}\leqslant\left(\dfrac{\omega}{m}\right)^{1/2} & \text{for } \omega\gg\eta \quad (24)\\[2ex] \dfrac{|\epsilon_1-\epsilon_2|}{\omega}\leqslant\left(\dfrac{\eta^2}{\omega m}\right)^{1/2} & \text{for } \omega\ll\eta. \quad (25)\end{cases}$$

IV. THE REGION OF DOMINATION OF FINAL STATE INTERACTION

If $\epsilon_{1,2}\gg J$ the amplitude is determined by the FSI until we are not too close to the center of the distribution—see [1] and Sec. III of the present paper.

The process passes through the intermediate state in which the system consists of a free electron and ion He^+. The latter can be in an excited or the ground state. Starting with the case of the function $\Psi(r_1,r_2)$ being presented through the single-electron functions $[\Psi(r_1,r_2)=\psi(r_1)\psi(r_2)$ in the case of helium] we present the amplitude as (see Fig. 2)

$$F=\int\frac{d^4f}{(2\pi)^4i}\sum_k\langle\varphi_2|V_B|\varphi^{(k)}\rangle\langle\varphi^{(k)}|V_A|\Psi\rangle\frac{1}{f_0-\omega_k+i\delta}\times\frac{1}{\omega-J-f_0-\dfrac{(p-f)^2}{2m}+i\delta}F_\gamma. \tag{26}$$

Here $\varphi^{(k)}$ denote the states of He^+ with the energies of excitations over the ground state ω_k. Block A describes the interaction V_A in the ion caused by removing the fast electron. In the shake-off approximation $V_A=1$. Block B stands

for scattering of the ionized electron on the ion in the state $|\varphi^{(k)}\rangle$ and F_γ is the amplitude of the single photoeffect—see Eq. (9).

The integral in the right-hand side of Eq. (26) can be evaluated as the sum of the residues at the points $f_0=\omega_k$. Since only the states with $\omega_k\sim J$ are important (the wave functions of the higher ones are suppressed), the propagator of the free electron does not depend on ω_k, as its denominator is of the order $p_0\eta/m\gg J$. Thus the sum over $|\varphi^{(k)}\rangle$ can be calculated by closure, leading to

$$F=\int \frac{d^3f}{(2\pi)^3}\langle\varphi_2|V_B|\psi\rangle\frac{1}{\epsilon_1+\epsilon_2-\dfrac{(p-f)^2}{2m}}. \tag{27}$$

Since $\epsilon_2\gg J$

$$\langle\varphi_2|V_B|\psi\rangle=F_{ee}(\omega,\epsilon_2)\psi(f) \tag{28}$$

with F_{ee} the amplitude of the inelastic scattering of the free electron with the energy ω on that at rest while the energy of the secondary electron becomes ϵ_2. As $\epsilon_2\gg J$, the latter amplitude can be treated in the lowest order of perturbative theory. Thus the amplitude is

$$F=-F_\gamma(P)F_{ee}(\omega,\epsilon_2)\times 2m\mu(p_0,P) \tag{29}$$

with

$$\mu(p_0,P)=\int\frac{d^3f}{(2\pi)^3}\psi(f)\frac{1}{(P-f)^2-p_0^2}. \tag{30}$$

The function $\mu(p_0,P)$ has a sharp maximum at $P=p_0$. Really, Eq. (30) can be presented as

$$\mu(p_0,p)=\frac{1}{4\pi}\int d^3r\psi(r)\frac{1}{r}e^{-i(\vec{p}\vec{r})+ip_0r}. \tag{31}$$

Since $P,p_0\gg\eta$, while important values of r are of the order η^{-1}, we can evaluate Eq. (31) as

$$\mu(p_0,\Delta)=\frac{i}{2p_0}\int\psi(r)e^{i\Delta r}dr \tag{32}$$

with $\Delta=p_0-P$.

Putting $P=p_0$ in the argument of the amplitude F_γ we obtain

$$\frac{d\sigma^{2+}(\omega)}{d\epsilon_2}=\sigma^+(\omega)\frac{d\sigma_{ee}(\omega_1,\epsilon_2)}{d\epsilon_2}\kappa \tag{33}$$

with σ_{ee} the cross section of the scattering of the free electron with the energy ω on the free one at rest. The last factor involved is

$$\kappa=4p_0^2\int\frac{d\Delta}{2\pi}|\mu(p_0,\Delta)|^2. \tag{34}$$

Using Eq. (32) we find

$$\kappa=\int drdr'\frac{d\Delta}{2\pi}\psi(r)\psi^*(r')e^{i\Delta(r-r')} \tag{35}$$

leading to [20]

$$\kappa=\frac{\langle\psi|r^{-2}|\psi\rangle}{4\pi}. \tag{36}$$

A similar analysis leads to the expression for the energy distribution for the more general form of the function $\Psi(r_1,r_2)$:

$$\frac{d\sigma^{2+}(\omega)}{d\epsilon_2}=\sigma^+(\omega)\frac{d\sigma_{ee}(\omega,\epsilon_2)}{d\epsilon_2}\frac{\langle r^{-2}\rangle}{4\pi} \tag{37}$$

with

$$\langle r^{-2}\rangle\equiv\frac{\langle\Psi(0,r)|r^{-2}|\Psi(0,r)\rangle}{N_0^2}. \tag{38}$$

It is sufficient to put

$$\frac{d\sigma_{ee}}{d\epsilon_2}=\frac{\pi\alpha^2}{\omega}\left(\frac{1}{\epsilon_2}+\frac{1}{\omega-\epsilon_2}\right)^2. \tag{39}$$

V. THE CENTRAL REGION

If the energies of the outgoing electrons do not differ much, the process can take place with small momentum $q\lesssim\eta$ transferred to the nucleus. Thus both bound electrons are at the distances $r\sim\eta^{-1}$ from the nucleus. This causes a strong enhancement in the energy distribution.

In this section we calculate the distribution of electrons at $|\epsilon_1-\epsilon_2|\ll\omega$. Assuming $\epsilon_1>\epsilon_2$ we introduce the variable

$$\beta=\frac{\epsilon_1-\epsilon_2}{\omega}=1-\frac{\epsilon_2}{\omega/2},\quad \beta\ll 1, \tag{40}$$

which describes the distance of the value of the electron energies from the center of the energy distribution. The electron energies and momenta are

$$\epsilon_i=\frac{\omega}{2}(1\pm\beta),\quad p_i^2=p^2(1\pm\beta),\quad p^2=m\omega. \tag{41}$$

In order to calculate the energy distribution in the whole region $\beta\ll 1$ note that at $\beta\sim 1$, $q\sim p$ the amplitude is dominated by its imaginary part, see Eqs. (29) and (32), while the real part can be neglected. At $\beta\ll 1$, $q\ll p$ the real part is strongly enhanced while the imaginary part is of the same order as at $\beta\sim 1$. Thus the contribution of the imaginary part of the amplitude is presented by Eq. (37) at all values of β, coming from integration over large $q\sim p$. Thus to obtain the energy distribution at $\beta\ll 1$ one should add the contribution of the real part of the amplitude integrated over $q\ll p$. The enhancement of the distribution is most effective for the values of β limited by Eqs. (24) and (25) when $q\lesssim\eta$. However, to match the two contributions one has to consider larger values of β for which still $\beta\ll 1$.

Hence we present the energy distribution as

$$\frac{d\sigma^{2+}}{d\epsilon_2}=\left(\frac{d\sigma^{2+}}{d\epsilon_2}\right)_{\ell}+\left(\frac{d\sigma^{2+}}{d\epsilon_2}\right)_s. \tag{42}$$

Here the first term is caused by large momentum transferred $q\sim p\gg\eta$. It is described by Eq. (37). The second term is determined by small momentum $q\ll p$.

In this section we find the energy distribution $d\sigma^{2+}/d\epsilon$ ($\epsilon\equiv\epsilon_2<\omega/2$) as a function of $\beta=1-\epsilon/(\omega/2)$ at $\beta\ll 1$. Special attention will be devoted to the intervals of the values of β limited by Eqs. (24) and (25). For the contribution $(d\sigma^{2+}/d\epsilon)_{\not}$ we immediately write

$$\frac{1}{\sigma^+}\left(\frac{d\sigma^{2+}}{d\epsilon}\right)_{\not}=\frac{4\alpha^2\langle r^{-2}\rangle}{\omega^3}(1+2\beta^2); \tag{43}$$

see Eqs. (37)–(39).

It is convenient to present the cross section as

$$d\sigma^{2+}=\frac{\pi}{\omega}\delta(\epsilon_1+\epsilon_2-\omega)|F|^2\frac{d^3p_2}{(2\pi)^3}\frac{d^3q}{(2\pi)^3} \tag{44}$$

with the contribution $(d\sigma^{2+}/d\epsilon)_s$ coming from integration over $q\sim\eta\ll p$. The latter limit causes the dependence of the values of the energies of the outgoing electrons on the other variables. We find from Eq. (6)

$$\epsilon_1-\epsilon_2=-\frac{(p_2k)}{m} \tag{45}$$

if $\omega=|k|\gg\eta$ and

$$\epsilon_1-\epsilon_2=-\frac{(p_2q)}{m} \tag{46}$$

if $\omega=|k|\ll\eta$—see Eqs. (24) and (25).

Describing the intermediate and final state electrons by the free functions we present the general form of the amplitude as

$$F(k,p_i,q)=\int\frac{d^3f}{(2\pi)^2}\Psi(q-f,f)F_1(k,p_i,q,f) \tag{47}$$

with Ψ the initial state function, while the function F_1 contains the propagators carrying the large momenta $p_i\gg\eta$. At $q\sim\eta$ the integral over f is saturated by small $f\sim\eta$. The amplitude F depends on five independent variables composed of the vectors k, p_i, and q.

The limit $q\sim\eta\ll p$ yields additional ties between the variables of the amplitude. At $\omega\gg\eta$ we can put $q=f=0$ in the arguments of the amplitude F_1 as well as in Eq. (6). The amplitude F_1 becomes just that of the process with two free electrons at rest, F_0. The latter should depend on two variables, say ω and (p_2k). Thus

$$F(\omega,(p_2k),q^2)=S(q^2)F_0(\omega,(p_2k)) \tag{48}$$

with

$$S(q^2)=\int\frac{d^3f}{(2\pi)^3}\Psi(q-f,f). \tag{49}$$

Equation (48) appears to be true in the broader region

$$\omega\gg\eta(\alpha Z_V)^{1/2}\approx 700\ \text{eV}. \tag{50}$$

To prove the statement, consider the explicit form of the amplitude $F_1=F_{1b}+F_{1c}$ where the two terms correspond to the diagrams of Figs. 1(b) and 1(c):

$$F_{1b}=(4\pi\alpha)^{3/2}\sqrt{2}\frac{(ep_1)}{m}D(p_2-f)G_b(\epsilon_1-\omega,p_1-k)+(1\to 2),$$

$$F_{1c}=(4\pi\alpha)^{3/2}\sqrt{2}\frac{(e,q-f)}{m}D(p_2-f)G_c(\omega+J_1,k+q-f)+(1\to 2) \tag{51}$$

with $D(Q)=1/Q^2$ and $G(E,Q)=1/(E-Q^2/2m)$ the propagators of photon and free electron and $J_1<0$ the eigenvalue of the energy of the bound electrons. Putting $f=q=0$ we eliminate the term F_{1c}. The two terms of the amplitude F_{1b} cancel unless we take into account the corrections of the order $(p_ik)/m\omega$ in the expansions of the propagators $G_b\approx 1/\omega[1-(p_ik)/m\omega]$. To find the region of the values of ω where the account of finite values of q and f is more important than that of corrections $\sim(p_ik)/m\omega$ we put $k=0$ in the propagators of the electrons. Neglecting the terms of the order $\eta^2/m\omega$ in the propagator G_c we find the amplitude F_1 to be proportional to the sum $(e,p_1-f)/(p_1-f)^2+(1\to 2)$. The latter changes sign under the transformation $f'=q-f$ and the integral in the right-hand side of Eq. (47) becomes zero. Thus the finite contribution is $(q/p)(\eta^2/m\omega)$ times smaller than each term in Eq. (51) for F_{1b}. This leads to the limit presented by Eq. (50). The explicit form of the amplitude is

$$F_0(\omega,(p_2k))=(4\pi\alpha)^{3/2}4\sqrt{2}\frac{(ep_2)(p_2k)}{m^3\omega^3}. \tag{52}$$

Now we calculate the energy distribution for the intervals of the values of the photon energies mentioned above. It is instructive to start with the larger values of ω.

A. The region of free kinematics $\omega\gg\eta\approx 6.3$ keV

The amplitude is described by Eq. (48) in which it is convenient to consider F_0 as a function of ω and β. Straightforward calculation gives

$$F_0(\omega,\beta)=(4\pi\alpha)^{3/2}\sqrt{2}\frac{4(ep_2)\beta}{m^2\omega^2}, \tag{53}$$

becoming zero at $\beta=0$. The latter can be easily seen from the general form of the amplitude

$$F_0(\omega,\beta)=(ep_1)f(\omega,\beta)+(ep_2)f(\omega,-\beta) \tag{54}$$

being proportional to $(ek)=0$ at $\beta=0$. This leads to

$$\frac{1}{\sigma^+}\left(\frac{d\sigma^{2+}}{d\epsilon}\right)_s=\frac{12\sqrt{2}}{mZ^2}\left(\frac{m}{\omega}\right)^{3/2}\left(1-\frac{m\beta^2}{\omega}\right)\beta^2C, \tag{55}$$

with

$$C=\frac{1}{N_0^2}\int\frac{d^3q}{(2\pi)^3}|S(q^2)|^2=\frac{1}{N_0^2}\int|\Psi(r,r)|^2d^3r, \tag{56}$$

the dimensionless number depending only on the characteristics of the initial state. It can be expressed through single-particle functions as

$$C=\frac{1}{N_0^2}\int |\psi(r)|^4 d^3r. \tag{57}$$

In the special case of hydrogenlike functions $C=1/8$ for any value of Z.

The distribution $(d\sigma^{2+}/d\epsilon_2)_s$ becomes finite at $\beta^2\to 0$ if finite values of q are taken into account in Eq. (6). The equation becomes more complicated; for the order of magnitude estimation the factor β^2 in the right-hand side of Eq. (55) should be replaced by η^2/ω^2 at $\beta^2 \ll J/\omega$. Note that the distribution becomes zero at the end points of the interval described by Eq. (24), matching $(d\sigma^{2+}/d\epsilon_2)_{\not\ell}$—see Eq. (43).

Comparing Eqs. (43) and (55) one can see that at $\beta^2=(1/2)(\omega/m)$ where $(d\sigma^{2+}/d\epsilon)_s$ reaches its maximum value the contribution is more than 10^3 times larger than that of $(d\sigma^{2+}/d\epsilon)_{\not\ell}$.

B. The dipole approximation region $\omega \ll \eta$ [but still $\omega \gg \eta_1 \equiv \eta(\alpha Z_V)^{1/2} \approx 700$ eV]

In this region we can neglect momentum k in Eq. (6). Thus the limits for q are

$$2p^2(1-\sqrt{1-\beta^2}) \le q^2 \le 2p^2(1+\sqrt{1-\beta^2}), \tag{58}$$

which gives at $\beta \ll 1$

$$p\beta \le q \le 2p. \tag{59}$$

In this region Eq. (52) for the amplitude is still true. We express the energy ϵ_1 through ϵ_2 and $(p_2 q)$ [Eq. (46)] and use the δ function in Eq. (44) for the integration over the azimuthal angle of the vector q. The distribution is

$$\frac{1}{\sigma^+}\left(\frac{d\sigma^{2+}}{d\epsilon dt}\right)_s=\frac{12\sqrt{2}}{Z^2}\left(\frac{\omega}{m}\right)^{1/2} t^2(1-t^2)H(p\beta) \tag{60}$$

with $p=(m\omega)^{1/2}$, $t=(p_2 k)/p_2 k$,

$$H(p\beta)=\frac{1}{N_0^2}\int_{p\beta}^{\infty}\frac{dq\, q}{2\pi^2}|S(q)|^2, \tag{61}$$

while $S(q)$ is defined by Eq. (49). We replaced the upper limit of integration by infinity since the integral over q is saturated by $q \ll p_i$.

To deal with dimensionless functions we introduce $\phi(p\beta)=\eta H(p\beta)$ and thus

$$\frac{1}{\sigma^+}\left(\frac{d\sigma^{2+}}{d\epsilon}\right)_s=\frac{16\sqrt{2}}{5Z^2}\left(\frac{\omega}{m}\right)^{1/2}\frac{1}{\eta}\,\phi(p\beta) \tag{62}$$

with $p=(m\omega)^{1/2}$. In the argument of the function ϕ the value $p\beta$ is compared to the characteristic momentum of the bound electron. Equation (61) shows ϕ to be a decreasing function of β. Presenting

$$\phi(p\beta)=\phi_0-\phi_1(p\beta), \quad \phi_0=\phi(0), \tag{63}$$

we find

$$\phi_0=\phi(0)=\frac{1}{N_0^2}\frac{\eta}{2\pi^2}\int d^3r d^3r'\,\psi(r,r)\frac{1}{|r-r'|^2}\Psi(r',r') \tag{64}$$

and

$$\phi_1(p\beta)=\frac{1}{N_0^2}\frac{\eta}{\pi^2}\int d^3r d^3r'\,\psi(r,r)\times\frac{\sin^2(p\beta|r-r'|/2)}{|r-r'|^2}\Psi(r',r'). \tag{65}$$

These equations show how

$$\phi(p\beta)=\frac{\eta}{2\pi^2 N_0}\int d^3r d^3r'\,\psi(r,r)\frac{\cos p\beta|r-r'|}{|r-r'|^2}\Psi(r',r') \tag{66}$$

vanishes smoothly at $\beta\sim 1$.

In the very vicinity of the center of the energy distribution, at $\beta \ll (J/\omega)^{1/2}$, we obtain

$$\phi_1(p\beta)=\frac{1}{4}\left(\frac{p\beta}{\eta}\right)^2\mu,\ \mu=\frac{\eta^3 h^2}{N_0^2\pi^2},$$

$$h=\int d^3r\Psi(r,r). \tag{67}$$

If $\psi(r,r)$ is the product of single-particle functions we find $h=1$.

Comparing Eqs. (43) and (62) we see that in the while region $\omega \gg \eta_1=\eta(\alpha Z_V)^{1/2}$ the total distribution $(1/\sigma^+)(d\sigma^{2+}/d\epsilon)$ reaches a local maximum at the point $\beta=0$. The contribution $(d\sigma^{2+}/d\epsilon)_s$ exceeds $(d\sigma^{2+}/d\epsilon)_{\not\ell}$ at larger energies ω since β^2 enters the function ϕ being multiplied by the large factor $p^2/\eta^2 \gg 1$. One can see that $(d\sigma^{2+}/d\epsilon)_s \gg (d\sigma^{2+}/d\epsilon)_{\not\ell}$ if $\omega \gg \eta(\alpha Z)^{3/7}\sim 1.3\eta_1 \sim 1$ keV.

To illustrate the matching of the two terms of Eq. (42) consider the region $1 \gg \beta \gg (J/\omega)^{1/2}$. Since here $q > \beta p \gg \eta$ we can obtain

$$S(q)=N_0\psi(q)=N_0^2\frac{8\pi\eta}{q^4} \tag{68}$$

and Eq. (42) takes the form

$$\frac{1}{\sigma^+}\frac{d\sigma^{2+}}{d\epsilon_2}=\frac{4\alpha^2}{\omega^3}\left[\langle r^{-2}\rangle(1+2\beta^2)+\frac{64\sqrt{2}}{15}\frac{N_0^2}{m}\left(\frac{\omega}{m}\right)^{1/2}\frac{1}{\beta^6}\right]. \tag{69}$$

The distribution reaches its minimum at $\beta=\beta_0$ with

$$\beta_0^8=\frac{32\sqrt{2}}{5}\frac{N_0^2}{\langle r^{-2}\rangle m}\left(\frac{\omega}{m}\right)^{1/2}. \tag{70}$$

Thus Eq. (70) indeed determines the point $\beta_0 \ll 1$. Note that β_0 depends on ω very weakly.

We conclude this subsection by adducing the function ϕ calculated with hydrogenlike functions of the initial state,

$$\phi(p\beta)=\frac{1}{3\pi}\left(\frac{4\eta^2}{p^2\beta^2+4\eta^2}\right)^3. \tag{71}$$

In this model $\beta_0\approx 0.5$; the energy distribution in the central region is dominated by $(1/\sigma^+)(d\sigma^{2+}/d\epsilon)_s$ at $\omega\gtrsim 2.5$ keV.

C. The region $\omega\approx\eta\approx 6.3$ keV

Keeping both k and q finite in Eq. (6) we find now

$$q\lesssim\beta p+\omega t. \tag{72}$$

Thus the distribution of outgoing electrons is described by Eq. (60) with $H(p\beta)$ being replaced by $H(p\beta+\omega t)$.

Now we see how the maximum of the distribution $(d\sigma^{2+}/d\epsilon)_s$ at $\beta=0$ for $\omega\ll\eta$ converts into a minimum at $\omega\gg\eta$. Putting $\omega\gg\eta$ we find that at $|t|\sim 1$ q can be made as small as η only if the two terms in the right-hand side of Eq. (72) do compensate each other to a large extent. Thus the limits of the values of t become a function of ω and β with $t\to 0$ at $\beta\to 0$. This leads to the zero value of the distribution at $\omega\gg\eta$ and $\beta\to 0$.

D. The region $\omega\lesssim\eta(\alpha Z_V)^{1/2}\approx 700$ eV

This is the part of the dipole approximation region in which many of the earlier experiments were carried out. We start the analysis with the case $\omega\ll\eta_1=\eta(\alpha Z_V)^{1/2}$ when the amplitude is the result of strong cancellation between the contributions of the terms F_{1b} and F_{1c} presented by Eq. (51). It does not vanish due to the finite difference between the propagators $G_b=1/\omega$ and $G_c=1/[\omega+J_1-(q-f)^2/2m]$. The amplitude of the process is

$$F=(4\pi\alpha)^{3/2}\frac{2\sqrt{2}}{m^2\omega^3}\,T(q) \tag{73}$$

with

$$T(q)=\int\frac{d^3f}{(2\pi)^3}\,\psi(q-f,f)\left(\frac{f^2}{2m}-J_1\right)(ef) \tag{74}$$

leading to the distribution

$$\frac{1}{\sigma^+}\left(\frac{d\sigma^{2+}}{d\epsilon}\right)_s=\frac{4\sqrt{2}}{\omega^3}\frac{1}{Z^2N_0^2}\,R(p,\beta) \tag{75}$$

with

$$R(p,\beta)=\int_{p\beta}^{2p}\frac{dq\;q^3}{2\pi^2}|J(q)|^2, \tag{76}$$

while the function

$$J(q)=\int d^3r e^{i(qr)}U(r)\left(1-\frac{i(q\nabla)}{4q^2}\right)\Psi(r,r) \tag{77}$$

originates from Eq. (74) with $U(r)$ the potential energy of the atom at the point r.

To deal with dimensionless functions, introduce

$$V(q)=\frac{m}{\eta^3}\,qJ(q),\quad \Lambda(p,p\beta)=\frac{\eta}{N_0^2}\int_{p\beta}^{2p}\frac{dq\;q}{2\pi^2}|V(q)|^2. \tag{78}$$

At $q\approx\eta$, $\beta\lesssim(J/\omega)^{1/2}$, V and Λ are of the order of unity. Equation (75) takes the form

$$\frac{1}{\sigma^+}\left(\frac{d\sigma^{2+}}{d\epsilon}\right)_s=\frac{4\sqrt{2}\eta^4}{m^2\omega^3Z^2}\frac{\eta}{p}\,\Lambda(p,p\beta). \tag{79}$$

Comparing Eqs. (43) and (79) we find

$$\left(\frac{d\sigma^{2+}}{d\epsilon}\right)_s\sim\left(\frac{\omega}{J}\right)^{1/2}\left(\frac{d\sigma^{2+}}{d\epsilon}\right)_{\ell}\lesssim\left(\frac{d\sigma^{2+}}{d\epsilon}\right)_{\ell}.$$

We shall see how the account of $(d\sigma^{2+}/d\epsilon)_s$ in the total energy distribution

$$\frac{1}{\sigma^+}\frac{d\sigma^{2+}}{d\epsilon}=\frac{4\alpha^2\eta^2}{\omega^3}\left[\frac{\langle r^{-2}\rangle}{\eta^2}(1+2\beta^2)+2\left(\frac{\eta^2}{2m\omega}\right)^{1/2}\left(\frac{\eta}{m\alpha Z}\right)^2\Lambda(p,p\beta)\right] \tag{80}$$

influences the $1+2\beta^2$ law of the first term.

Note first that the shape of the spectrum curve in the very vicinity of the center $\beta\to 0$ is determined by the first term of Eq. (80). One can see this by presenting

$$\Lambda(p,p\beta)=\Lambda(p,0)-\Lambda_1(p\beta) \tag{81}$$

and finding $\Lambda_1\sim\beta^4$ at $p\beta\ll\eta$ since $V(0)=0$—see Eq. (78). Equation (78) shows that $\Lambda(p,p\beta)$ is growing while ϵ approaches $\omega/2$, i.e., while β diminishes. Thus the second term in Eq. (80) makes the spectrum curve flatter than the parabola $1+2\beta^2$. One can see from Eq. (78) that the effect is of the same strength in the whole region $\beta\ll 1$, vanishing smoothly when β approaches unity—see Eq. (58).

To find the dependence on ω of the influence of the contribution of the second term on the shape of the curve it is instructive to analyze the function $\Lambda(p,p\beta)$ in the center of the energy distribution $\beta=0$. The general form of $\Lambda(p,p\beta)$ can be obtained by considering $x=p\beta\gg\eta$. This yields $q\gg\eta$ where

$$T(q)=\frac{4\pi\eta N_0^2}{q^2m}(eq),\quad V(q)=4\pi\frac{N_0^2}{\eta}\frac{1}{q^2}, \tag{82}$$

leading to

$$\Lambda(p,x)=4\frac{N_0^2}{\eta^3}\left[\ln\frac{4p^2}{x^2}+0\left(\frac{\eta^2}{x^2}\right)\right] \tag{83}$$

and to the general equation

$$\Lambda(p,p\beta)=4\frac{N_0^2}{\eta^3}\left[\ln\frac{p^2}{\eta^2}-\lambda\left(\frac{p\beta}{\eta}\right)\right] \tag{84}$$

with $\lambda\sim\ln(p\beta/\eta)$ if $p\beta\gg\eta$. Returning to Eq. (80) we find the influence of the second term to increase with ω while

$$\ln\frac{p^2}{\eta^2}<2+\lambda(0). \tag{85}$$

The value $\lambda(0)$ depends on the initial state wave function.

For hydrogenlike functions we find

$$\Lambda(p,p\beta)=\frac{4}{\pi}\left(\ln\frac{p^2}{\eta^2}+\ln X-\frac{5}{3}X+\frac{7}{18}X^2-\frac{1}{27}X^3\right) \tag{86}$$

with $X(p\beta)=4\eta^2/(p^2\beta^2+4\eta^2)$. This leads to $\lambda(0)\approx 1.3$. Thus the effect of flattening of the spectrum curve increases with the value of the photon energy while $\omega\lesssim 1.3$ keV.

Now we turn to the case $\omega\sim\eta_1\equiv\eta(\alpha Z_V)^{1/2}$ where the two contributions to the amplitude described by Eqs. (52) and (73) are of the same order of magnitude. Since the integration over the direction of the vector q in Eq. (44) eliminates the interference between the two terms we write for the energy distribution

$$\frac{1}{\sigma^+}\frac{d\sigma^{2+}}{d\epsilon}=\frac{4\alpha^2\eta^2}{\omega^3}\left[\frac{\langle r^{-2}\rangle}{\eta^2}(1+2\beta^2)+2\left(\frac{\eta^2}{2m\omega}\right)^{1/2}\times\Lambda(p,p\beta)+\frac{4\sqrt{2}}{5}\frac{1}{(\alpha Z)^2}\left(\frac{\omega}{m}\right)^{1/2}\left(\frac{\omega}{\eta}\right)^3\phi(p\beta)\right]. \tag{87}$$

Here the first term in the square brackets comes from $(1/\sigma^+)(d\sigma^{2+}/d\epsilon)_{\not}$, while the second and the third come from $(1/\sigma^+)(d\sigma^{2+}/d\epsilon)_s$. Using Eqs. (62) and (79) we find that at a certain value of the photon energy

$$\omega=\omega_1\equiv c\,\eta(\alpha Z_V)^{5/9}\simeq c\,\eta_1\times 0.79 \tag{88}$$

the character of the spectrum curve changes. At $\omega>\omega_1$ it reaches a local maximum at the point $\beta=0$. The coefficient c is related to the parameters of the initial state wave function by a rather clumsy relation

$$c=\left(5\times 2\sqrt{2}\pi\times\frac{\pi N_0^2}{\eta^3}\times\frac{\langle r^{-2}\rangle}{2\eta^2}\times h^2\right)^{2/9} \tag{89}$$

—see Eq. (67) for h. Note that at $\omega=\omega_1$ the second and the third terms of Eq. (87) obtain extra factors $(\alpha Z_V)^{2/9}$ and $(\alpha Z_V)^{4/9}$ with respect to the first term.

For the hydrogenlike functions of the initial state the three last factors in the parentheses of Eq. (89) become unity. This leads to $c=2.3$. Thus in this model the character of the spectrum curve changes at $\omega\approx 1.5$ keV.

VI. THE OUTLOOK OF THE ENERGY DISTRIBUTION IN HELIUM

Now we can have a general view of the energy distribution. Starting with the values of $\epsilon_2\lesssim J$ we increase the energy ϵ_2, observing the replacement of the GSI mechanism by that of the FSI.

Where does the replacement take place? Strictly speaking we must calculate the total contribution of the FSI giving the correction of the order J/ω to the GSI contribution. A consistent way of calculating the FSI correction to shake-off-type processes was described in Ref. [21]. One must calculate

$$\frac{1}{\sigma^+}\frac{d\sigma^{2+}}{d\epsilon_2}\sim\frac{J}{\omega}\left(\langle\varphi_2|\psi\rangle\left\langle\psi\left|r_0\frac{d}{dr}\right|\varphi_2\right\rangle-\langle\varphi_2|\psi\rangle\times\langle\psi|\ln^2(r-r_z)|\varphi_2\rangle+|\langle\varphi_2|\ln(r-r_z)|\psi\rangle|^2\right) \tag{90}$$

with the z axis direction being that of the fast electron momentum p_1 and r_0 the Bohr radius.

To feel the size of the effect one can try, however, the simplest equation, which just includes the interaction of the secondary electron with the bare nucleus of helium,

$$\frac{1}{\sigma^+}\frac{d\sigma^{2+}}{d\epsilon_2}=\frac{\langle r^{-2}\rangle}{4\pi}\frac{N(\xi_2)}{(\epsilon_2+J^+)^2}\frac{\pi\alpha^2}{\omega} \tag{91}$$

with $\xi_2=(J^+/\epsilon_2)^{1/2}$ while J^+ is the ionization potential of the ion He^+ and

$$N(\xi_2)=\frac{2\pi\,\xi_2}{1-\exp(-2\pi\xi_2)}\exp(-4\xi_2\cot^{-1}\xi_2). \tag{92}$$

Equation (91) approximates the right-hand side (RHS) of Eq. (90) if we assume the overlap integral $\langle\varphi_2|\psi\rangle$ to be an additional small parameter. In this case the RHS of Eq. (90) is dominated by the last term.

One can see that the smaller are the values of ω the sooner the replacement takes place. The values of ϵ_2 where the replacement occurs depend on the model used for the ground state function. Comparing Eq. (91) to the energy distribution caused by the GSI in the perturbation theory model [1] we find the two mechanisms to give the contribution of the same order at $\epsilon_2\sim 30$ eV for all the photon energies $\omega\lesssim 5$ keV. At larger values of ϵ_2 the FSI term dominates.

Certainly more realistic models of the GSI can change the numbers. However, the main result of the analysis, the early replacement of the GSI mechanism by that of the FSI, remains the same. The reason is that the FSI contribution contains the small factor $(J/\omega)^2$ and the GSI term also contains the small factor $|\langle\varphi_2|\psi\rangle|^2$.

Now let us increase the value of ϵ_2, moving to the center of the spectrum. While we keep $\omega\lesssim 1$ keV the spectrum curve drops monotonically, being described by Eq. (87). The dependence of the energy distribution on $\beta=1-\epsilon_2/(\omega/2)$ is expected to be flatter than the $1+2\beta^2$ parabola of the first term. The effect of flattening increases with ω. The interval of the values of β where the phenomenon manifests itself does not depend on ω. At $\omega_1\sim\eta(\alpha Z)^{5/9}$ the character of the curve changes and it obtains a local maximum at $\beta=0$. We expect the value to be about 1.5 keV. At this point the distribution is still dominated by the first term of Eq. (87). Thus the maximum is a broad and low one. However, due to the strong dependence of the third term of Eq. (87) on ω, at $\omega\gtrsim 1.7\omega_1$ the latter dominates the distribution at $\beta\lesssim(J/\omega)^{1/2}$.

Increasing the value of ω but still keeping $\omega\lesssim\eta\approx 6$ keV we find the spectrum curve growing strongly in the region $\beta\lesssim(J/\omega)^{1/2}$. The positions of the points β_0 where the distribution reaches the minimum value are estimated by Eq. (70). The values of β_0 vary slowly with ω. The magnitude of

the relative enhancement in the center of distribution increases quickly with ω—Eqs. (43) and (62).

Note that until we deal with the energies $\omega \ll \eta \approx 6.5$ keV the size of the region of quasifree kinematics grows as $\omega^{1/2}$. Its relative part $|\beta|$ falls as $\omega^{-1/2}$, reaching the smallest value $|\beta| = (\alpha Z_V)^{1/2} \approx 0.11$ at $\omega = \eta$.

At $\omega \approx \eta \approx 6.3$ keV the equations for the energy distribution are rather complicated—see Sec. V. But at $\omega > \eta$ corrections to Eq. (55) are of the order η^2/ω^2. Thus, say, at $\omega = 12$ keV we can use Eq. (55) to describe the spectrum.

Equation (55) is true in the region of free kinematics determined by Eq. (24). The contribution matches that of the FSI, becoming zero at the borders of the region. The cross section changes rapidly in the interval. Say, at $\omega = 12$ keV its values at the points of maxima $\beta = (\omega/2m)^{1/2}$ are about 150 times larger than that on the borders of the region. The cross section diminishes if we make $|\beta|$ smaller. At $\beta = 0$ the value is four times smaller than that on the borders of the interval.

If $\omega \gg \eta$ the size of the central region grows as $\omega^{3/2}$ while the distribution $(1/\sigma^+)(d\sigma^{2+})/(d\epsilon_2)$ diminishes as $\omega^{-1/2}$. The contribution of the region to the total cross section is of the order $\sigma^+ \omega/m$. Thus at the values $\omega \sim m \approx 500$ keV the region contributes a value of the same order as the edge region. The case $\omega \sim m$ was considered in Ref. [22].

VII. THE OUTLOOK OF ENERGY DISTRIBUTION IN HEAVIER ATOMS

Let us see how the whole picture is modified for the case of double photoionization of an atom with the charge of the nucleus Z.

In the case of two external electrons experiencing the effective charge $Z_{eff} \approx 1$ we find $\eta_{eff} \approx m\alpha = 3.7$ keV in the edge region and in the FSI domination region the cross section σ^{2+} is singled out as a factor in a natural way since in the distribution $d\sigma^{2+}/d\epsilon$ both values depend on Z in the same way. Since [23] $N_0^2 \equiv |\psi(r=0)|^2 \sim Z$ they are proportional to Z^3—see Eq. (13). On the other hand, in the central region the distribution depends on Z_{eff} rather than on Z. Thus, the interplay between FSI and GSI mechanisms is the same as in helium until we come to the central region of the spectrum determined by Eqs. (24) and (25). Here the role of the small momentum transferred $q \sim \eta_{eff}$ is less important than in the case of helium. The relative contribution of the second term in the right-hand side of Eq. (42) is $(Z/Z_V)^3$ times smaller than in helium (recall that $Z_V = 27/16$). The contribution of $(d\sigma^{2+}/d\epsilon)_s$ becomes of the same order as that of $(d\sigma^{2+}/d\epsilon)_{\ell}$ at $\omega \sim 2(Z/Z_V)^{7/2}$ keV, i.e., $\omega \gg \eta_{eff}$. Hence the spectrum in the central region can be described by Eq. (42) with the two contributions to the right-hand side given by Eqs. (43) and (55).

The role of $(d\sigma^{2+}/d\epsilon)_s$ in the central region increases again if the orbital moments of both ionized states $\ell_{1,2} \neq 0$. Really in this case the cross sections in the edge region and in the FSI domination region contain σ^+ as a factor. The latter cross section is suppressed for $\ell \neq 0$. The GSI mechanism in the central region does not yield this quenching.

In the case of ionization of two K electrons we find $N_0^2 \sim Z^3$, $J \sim Z^2$, and $\eta_{eff} = m\alpha Z$; thus $\sigma^+ \sim Z^5$. Since the shake-off matrix element in the right-hand side of Eq. (17) drops as $1/Z$, we come to $d\sigma^{2+}/d\epsilon \sim Z^3$ in the edge region being proportional to Z^7 in the region of FSI domination. Thus the FSI mechanism replaces that of the GSI at smaller values of ϵ/J than in helium. In the central region the contribution of $(d\sigma^{2+}/d\epsilon)_s$ at $\omega \lesssim \eta_{eff}(\alpha Z)^{1/2}$ [Eqs. (75) and (79)] is proportional to Z^8. Thus the effect of flattening of the spectrum curve is stronger than in helium. It drops with ω as $\omega^{-1/2}$, while the contribution which increases with ω—Eq. (87)—contains the smaller factor Z^2. This leads to minor altering of the shape of the spectrum curve predicted by $(d\sigma^{2+}/d\epsilon)_{\ell}$ caused by the FSI in the whole region $\epsilon \gg J$ at larger values of ω.

VIII. THE ANGULAR DISTRIBUTION OF THE ELECTRONS

In the edge region the distribution is quite simple. The fast electron succeeds that of the single photoeffect while the slow one is the isotropic s wave.

In the two other regions of the spectrum we find a strong correlation between the directions of momenta of the two electrons. In the FSI region the maximum of the distribution over the angle θ_{12} between electron momenta $p_{1,2}$ is reached at $\theta_{12} = \pi/2$. The width of the maximum is $\eta/p \approx (J/\omega)^{1/2} \ll 1$. The dependence on the angles between p_i and $\bar{n} = \vec{k}/|k|$ is the same as in the single photoeffect with the electron's momentum $p_1 + p_2$. Thus in the region of domination of the FSI the distribution in $t_i = (p_i k)/p_i k$ is

$$\frac{d\sigma^{2+}}{d\epsilon dt} = \left(\frac{d\sigma^{2+}}{d\epsilon}\right) \times \frac{3}{8}\left[1 + \frac{\epsilon}{\omega} - t^2\left(\frac{3\epsilon}{\omega} - 1\right)\right] \tag{93}$$

with $d\sigma^{2+}/d\epsilon$ determined by Eq. (37).

At $\omega \ll 2$ keV the angular distribution is determined by Eq. (93) in the whole region $\epsilon_{1,2} \gg J$. At $\omega \gtrsim 2$ keV it is violated in the central region (Sec. V), being a more complicated interplay of several contributions if $\beta \leq (J/\omega)^{1/2}$. If $\omega \gg 2$ keV the directions of momenta of outgoing electrons are strongly correlated in the central region. The electrons move mostly in opposite directions, the value of the angle θ_{12} between p_1 and p_2 does not differ from π by more than $(J/\omega)^{1/2}$. The angular distribution in the central region takes the form [Eq. (60)]

$$\frac{d\sigma^{2+}}{d\epsilon dt} = \frac{d\sigma^{2+}}{d\epsilon} \times \frac{15}{4} t^2(1-t^2), \tag{94}$$

reaching maximum values if the values of the angles between p_i and k are $\pi/4$ or $3\pi/4$ (recall that $\theta \approx \pi$, $t_1 = -t_2$).

Note that at larger values of $\omega \gg \eta \approx 6.3$ keV the distribution of electrons in the central region is dominated by free kinematics which yields a certain relation between t and ϵ—Eq. (45). Thus

$$\frac{d\sigma^{2+}}{\sigma^+ d\epsilon dt} = \frac{12\sqrt{2}}{Z^2}\left(\frac{m}{\omega}\right)^{1/2} t^2(1-t^2)\,\delta\left(t - \frac{m\beta(\epsilon)}{p}\right) C \tag{95}$$

with $\beta(\epsilon) = 1 - \epsilon/(\omega/2)$, $\beta^2 \lesssim \omega/m$. Thus we expect the distribution $(1/\sigma^+)(d\sigma^{2+}/dt)$ to reach maximum values at

$$t^2(\epsilon)=\frac{m}{\omega}\beta^2(\epsilon). \tag{96}$$

The distribution $d\sigma^{2+}/dt$ integrated over ϵ again takes the form $t^2(1-t^2)$—Eq. (55). At $t=0$ and at $t=\pm 1$ the finite value is provided by the distribution of Eq. (93).

IX. SUMMARY

We analyzed the distribution of electrons in the double ionization of helium and heavier atoms. We calculated the cross section in the two regions of the spectrum corresponding to large energies of outgoing electrons $\epsilon_{1,2}\gg J$ discovered in Ref. [1] without specifying the model for the initial wave function $\Psi(r_1,r_2)$.

We show that at rather small values of the energies of the secondary electron ϵ_2 the ground state interaction mechanism is replaced by the final state one. The value of ϵ_2 where the replacement takes place becomes larger as the value of ω increases. The FSI contribution is presented in factorized form—Eq. (37). All the atomic physics effects are contained in the first two factors while the last one is of purely electrodynamical origin, describing the interaction of free electrons.

When the values of the energies of outgoing electrons are not too close to each other a large momentum should be transferred to the nucleus. Thus one of the electrons should approach the latter at distances much smaller than its classical orbit. When the values of $\epsilon_{1,2}$ become close enough—Eqs. (24) and (25)—it becomes sufficient to transfer small momentum to the nucleus. However, while sharing the energy transferred by photons the electrons should approach each other at small distances $r\sim(m\omega)^{-1/2}$. Note that this mechanism is caused by interaction in the ground state at $\omega\gg\eta(\alpha Z_v)^{1/2}\approx 700$ eV. At smaller energies it is the result of the strong cancellations between the contributions of the final state interaction and ground state interaction in the real part of the amplitude. For energies $\omega\lesssim\eta\approx 6$ keV the energy distribution is expressed through certain integrals depending on the form of the initial state wave function and on the energy of the outgoing electron—Eqs. (60), (62), and (75)–(79). In the very vicinity of the center of the energy distribution we can again single out certain factors depending only on the structure of the initial state—see, e.g., Eq. (67). Note that for $\omega\gg\eta\approx 6$ keV the energy distribution is also presented in factorized form containing an "electrodynamical factor" depending on ω and ϵ and an "atomic physics factor" depending only on parameters of the initial state wave function—Eq. (55).

The directions of momenta of outgoing electrons are strongly correlated. In the region of FSI domination the angle $\pi/2$ between p_1 and p_2 is preferred. In the central region they move mostly in opposite directions. In the region of FSI domination the angular distribution is expressed by Eq. (93). In the central region it is expressed by the factor $t^2(1-t^2)$ [see Eq. (94)] becoming zero at $t=0,\pm 1$.

In the heavier atoms the role of the FSI increases. If the charge of the nucleus Z is large enough the FSI can dominate in the whole region $\epsilon_i\gg J$—Sec. VII.

In Fig. 3 we show how the form of the spectrum of double photoionization of helium is modified when we change the value of ω. The figure illustrates the analyses presented in Sec. VI.

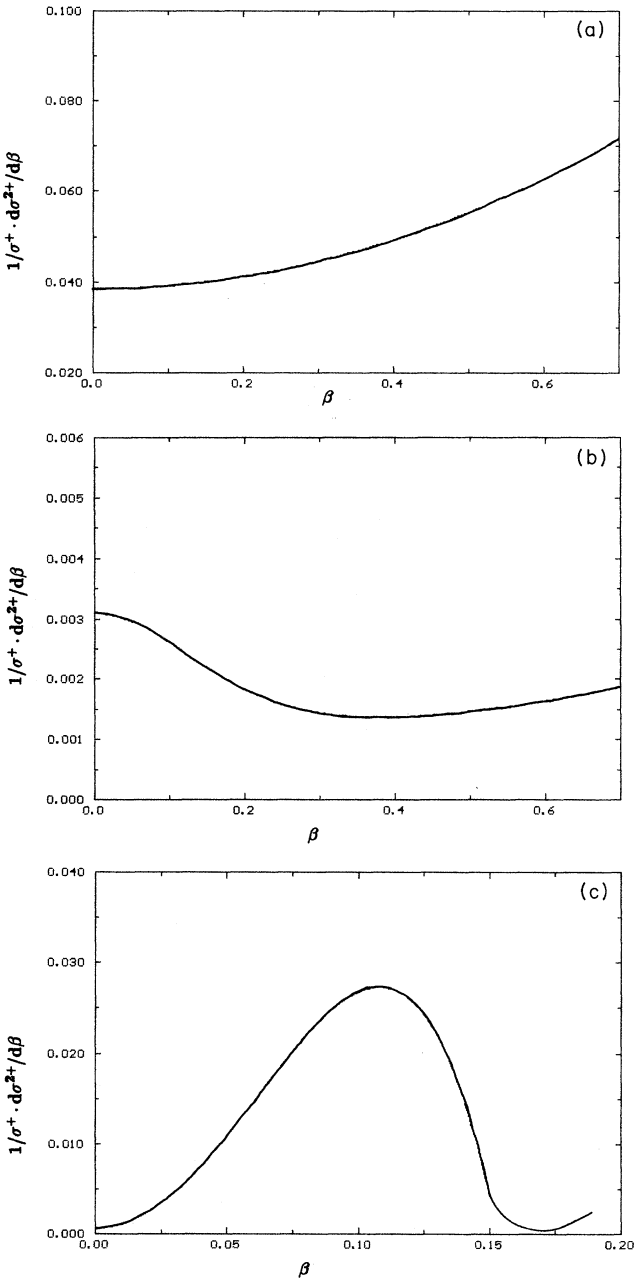

FIG. 3. The energy distribution $(1/\sigma^+)(d\sigma^{2+}/d\beta)=(\omega/2\sigma^+)(d\sigma^{2+}/d\epsilon)$ as a function of β. (a) corresponds to $\omega=500$ eV; (b) and (c) to $\omega=3$ keV and $\omega=12$ keV.

The distribution of outgoing electrons was analyzed in Refs. [5,6,9] where various precise wave functions were used for the description of initial and final states. Describing the outgoing electrons by plane waves, we may lose in accuracy as compared to [5,6,9]. However, we expect the approach to clarify certain general features of the distribution and the evolution of the shape of the spectrum curve with ω.

We find our results to be consistent with those obtained in [5,6,9] for several special values of the photon energy. In-

deed, the energy distributions in Fig. 5 of the paper by Hino *et al.* [5] show a flat part of the curve near the center of distribution. Its size increases while the value of photon energy increases from 200 eV to 500 eV and then to 1 keV. The effect of flattening also increases with ω. Both results are in agreement with those coming from our general analysis. Unfortunately, the scale used in the figure does not allow us to see if it reproduces the "fine structure" of the curve expected at $\omega=5$ keV.

The energy distributions obtained by Kornberg and Miraglia [6] for $\omega=1$ keV, 2 keV, and 3 keV shown in Fig. 2 of Ref. [6] also agree with our picture of evolution of the shape of the spectrum curve with ω. At $\omega=1$ keV the curve has a flat bottom, obtaining the flat top peaks at larger energies. Recall that we predict a change in the shape of the curve at values of ω between 1 keV and 2 keV. The values of $\beta=|(\epsilon_1-\epsilon_2)/\omega|$ where the curves for $\omega=2$ keV and $\omega=3$ keV reach the minimum value are practically the same, in agreement with our results. The peak is sharper for $\omega=3$ keV; this also coincides with the results of our calculations.

The energy distributions of outgoing electrons at $\omega=625$ eV and $\omega=2.8$ keV obtained by Teng and Shakeshaft [9] are presented by a curve with flat bottom in the first case and with a very flat top peak in the second case. The peak obtained in Ref. [6] for $\omega=2$ keV is sharper but this can be explained by the different wave functions of the initial state in Refs. [6] and [9]. The evolution of the shape of the curves with ω agrees with our results. Note also that in Ref. [9] a general analysis of the asymmetry coefficient at $\omega\approx 2$ keV was carried out. At these values of energies (i.e., at values close to the point of ω where the curve changes its shape) our limit equations (93) and (94) do not work in the central region. The results of analysis of the angular correlations of outgoing electrons in [9] support the earlier statement [1] that the regions $\theta_{12}\approx\pi/2$ and $\theta_{12}\approx\pi$ are singled out and shows it to be true also for calculations with more precise wave functions of the final state.

We expect the analysis carried out in the present paper to help us in approaching the other problems connected with double photoionization mentioned in the Introduction.

ACKNOWLEDGMENTS

I am happy to thank Professor A. Dalgarno, Professor U. Fano, and Professor R. H. Pratt for useful discussions. I am indebted to my colleagues at ITAMP for hospitality. My interest in the problem was renewed by discussions with Dr. N. B. Avdonina.

APPENDIX

Here we recall some of the features of the system of units and normalization scale used in Ref. [18]. Putting $\hbar=c=1$ we express all the velocities in units of that of light. The energies ϵ and ω of the electron and photon are related to their momenta p and k as

$$\epsilon=\frac{p^2}{2m}, \quad \omega=k. \tag{A1}$$

The velocity of the bound electron in the ground state of the hydrogenlike atom is αZ while the binding energy is $J=\eta^2/2m$ with $\eta=m\alpha Z$ the characteristic momenta of the K electron. The dipole approximation is true if $\omega=k\ll\eta$.

The single-electron wave functions are normalized in such a way that there is one particle per unit volume. This normalization condition is expressed by Eq. (16) of the text. The wave function of the free electron is

$$\varphi_p(r)=\exp[i(pr)]. \tag{A2}$$

Let us show how Eq. (12) of the text, which is Eq. (56.1) of Ref. [18] can be presented in the more traditional form of Eq. (69.5) of Ref. [16]. Indeed, Eq. (12) of the text can be presented as

$$d\sigma^+=\frac{\pi}{\omega}|\vec{F}_\gamma|^2 mp\,\frac{d\Omega}{(2\pi)^3} \tag{A3}$$

with

$$(\vec{F}_\gamma)_i=i\int d^3r\, e^{-i(pr)}\vec{\nabla}_i\psi(r)\frac{(4\pi\alpha)^{1/2}}{m}, \tag{A4}$$

while averaging over the polarization of the photon is implied. On the other hand, putting $\hbar=c=1$ in Eq. (69.5) of [16] we present it as

$$d\sigma^+=\frac{(2\pi)^2}{m^2\omega}|\vec{D}|^2 d\Omega \tag{A5}$$

with vector D defined by Eq. (59.3) of [16] as

$$D_i=i\sqrt{\frac{p}{m(2\pi)^3}}\int d^3r e^{-i(pr)}\nabla_i\psi(r), \tag{A6}$$

leading to the identity of Eqs. (A3) and (A5).

[1] M.Ya. Amusia, E.G. Drukarev, V.G. Gorshkov, and M.P. Kazachkov, J. Phys. B **8**, 1248 (1975).

[2] J.C. Levin, I.A. Sellin, B.M. Johansen, D.W. Lindle, R.D. Miller, N. Berrah, Y. Azuma, H.G. Berry, and D.H. Lee, Phys. Rev. A **47**, R16 (1993).

[3] T. Ishihara, K. Hino, and J.H. McGuire, Phys. Rev. A **44**, R6980 (1991).

[4] A. Dalgarno and H.R. Sadeghpour, Phys. Rev. A **46**, R3591 (1992).

[5] Ken-ichi Hino, T. Ishihara, F. Shimizu, N. Toshima, and J. McGuire, Phys. Rev. A **48**, 1271 (1993).

[6] M.A. Kornberg and J.E. Miraglia, Phys. Rev. A **48**, 3714 (1993).

[7] A.K. Kazansky and V.N. Ostrovsky, Phys. Rev. A **48**, R871

(1993).
[8] F. Maulbetsch and J.S. Briggs, Phys. Rev. Lett. **68**, 2004 (1992); J. Phys. B **26**, 1679 (1992).
[9] Z. Teng and R. Shakeshaft, Phys. Rev. A **47**, 3487 (1993); **49**, 3597 (1994).
[10] J.A.R. Samson, Phys. Rev. Lett. **65**, 2861 (1990).
[11] J.A.R. Samson, Ch.H. Greene, and R.J. Bartlett, Phys. Rev. Lett. **71**, 201 (1993).
[12] L.R. Andersson and J. Burgdörfer, Phys. Rev. Lett. **71**, 50 (1993).
[13] Ken-ichi Hino, P.H. Bergström, Jr., and J.H. Macec, Phys. Rev. Lett. **72**, 1621 (1994); T. Suric, K. Pisk, B.A. Logen, and R.H. Pratt, Phys. Rev. Lett. **73**, 790 (1994).
[14] J.H. McGuire, Adv. At. Mol. Opt. Phys. **29**, 217 (1991).
[15] A. Dalgarno and A.L. Stewart, Proc. Phys. Soc. London **76**, 49 (1960).
[16] H.A. Bethe and E.E. Salpeter, *Quantum Mechanics of One- and Two-Electron Atoms* (Plenum/Rosetta, New York, 1977).
[17] R.G. Newton, *Scattering Theory of Waves and Particles* (McGraw-Hill, New York, 1968).
[18] V.B. Berestetskii, E.M. Lifshitz, and L.P. Pitaevski, *Quantum Electrodynamics* (Pergamon, Oxford, 1982).
[19] J.D. Bjorken and S.D. Drell, *Relativistic Quantum Fields* (McGraw-Hill, New York, 1978).
[20] E.G. Drukarev, Yad. Fiz. **50**, 876 (1989) [Sov. J. Nucl. Phys. **50**, 546 (1989)].
[21] E.G. Drukarev and M.I. Strikman, Phys. Lett. B **186**, 1 (1987).
[22] E.G. Drukarev and F.F. Karpeshin, J. Phys. B **9**, 399 (1976).
[23] L.D. Landau and E.M. Lifshitz, *Quantum Mechanics* (Nauka, Moscow, 1973).